Accepted Manuscript

The synthesis and anticancer activity of 2-styrylquinoline derivatives. A p53 independent mechanism of action

Anna Mrozek-Wilczkiewicz, Michał Kuczak, Katarzyna Malarz, Wioleta Cieślik, Ewelina Spaczyńska, Robert Musiol

PII: S0223-5234(19)30477-5

DOI: https://doi.org/10.1016/j.ejmech.2019.05.061

Reference: EJMECH 11371

To appear in: *European Journal of Medicinal Chemistry*

Received Date: 8 February 2019

Revised Date: 21 May 2019

Accepted Date: 21 May 2019

Please cite this article as: A. Mrozek-Wilczkiewicz, Michał. Kuczak, K. Malarz, W. Cieślik, E. Spaczyńska, R. Musiol, The synthesis and anticancer activity of 2-styrylquinoline derivatives. A p53 independent mechanism of action, *European Journal of Medicinal Chemistry* (2019), doi: https://doi.org/10.1016/j.ejmech.2019.05.061.

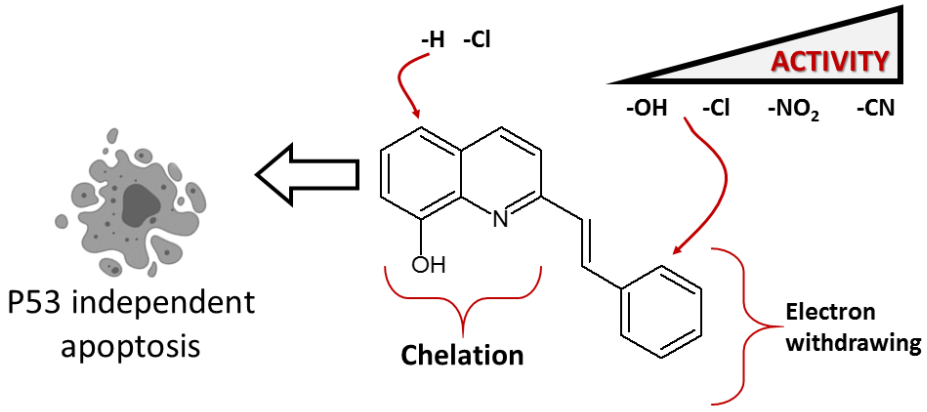

The synthesis and anticancer activity of 2-styrylquinoline derivatives. A p53 independent mechanism of action.

Anna Mrozek-Wilczkiewicz[a]*, Michał Kuczak[b], Katarzyna Malarz[a], Wioleta Cieślik[b], Ewelina Spaczyńska[b] and Robert Musiol[b]*

[a]A. Chełkowski Institute of Physics and Silesian Center for Education and Interdisciplinary Research, University of Silesia, 75 Pułku Piechoty 1a, 41-500 Chorzów, Poland

[b]Institute of Chemistry, University of Silesia, 75 Pułku Piechoty 1a, 41-500 Chorzów, Poland

*corresponding authors email: anna.mrozek-wilczkiewicz@us.edu.pl, robert.musiol@us.edu.pl

Keywords: 2-styrylquinoline derivatives, anticancer activity, p53 protein, reactive oxygen species, apoptosis, cell cycle inhibition

ABSTRACT

A series of styrylquinolines was designed and synthesized based on the four main quinoline scaffolds including oxine, chloroxine and quinolines substituted with a hydroxyl group or chlorine atom at the C4 position. All of the compounds were tested for their anticancer activity on wild-type colon cancer cells (HCT 116) and those with a p53 deletion. Analysis of SAR revealed the importance of electron-withdrawing substituents in the styryl part and chelating properties in the quinoline ring. The compounds that were more active were also tested on a panel of four cancer cell lines with mutations in *TP53* tumor suppressor gene. The results suggest that styrylquinolines induce cell cycle arrest and activate a p53-independent apoptosis. The apparent mechanism of action was studied for the most promising compounds, which produced reactive oxygen species and changed the cellular redox balance.

1. Introduction

Styrylquinoline (vinyl-quinoline) derivatives (SQ) are a group of aromatic and lipophilic compounds that have a broad spectrum of biological activity. They have been reported as being antibacterial [1][2], antiparasitic [3] and antiviral agents [4]. Styrylquinoline FZ-41 (**Fig. 1.**) entered clinical trials as an inhibitor of HIV integrase [5]. The antifungal

activity of SQ has also been broadly described [6–9] and the WK14 derivative was determined to be a selective inhibitor of the Cdr1p efflux pump [10]. More recently, their potency in neurodegenerative diseases has also been reported [11]. Their anticancer activity has been known for more than six decades since the works of Bahner [12,13] and Emmelot [14] were published. Unfortunately, the simple 2- and 4-styrylquinolines that were tested appeared to be rather non-selective and their cytotoxicity hampered their further development. Later, some more promising data has been revealed with a study on SQ that had been substituted with the carboxylic and hydroxyl groups in a quinoline moiety similar to FZ-41 [15]. Their lower lipophilicity correlated with a better solubility and selectivity. Several of these compounds appeared to be active at a micromolar level in colon cancers (HCT 116) as well as in neuroblastomas (SK-N-MC).

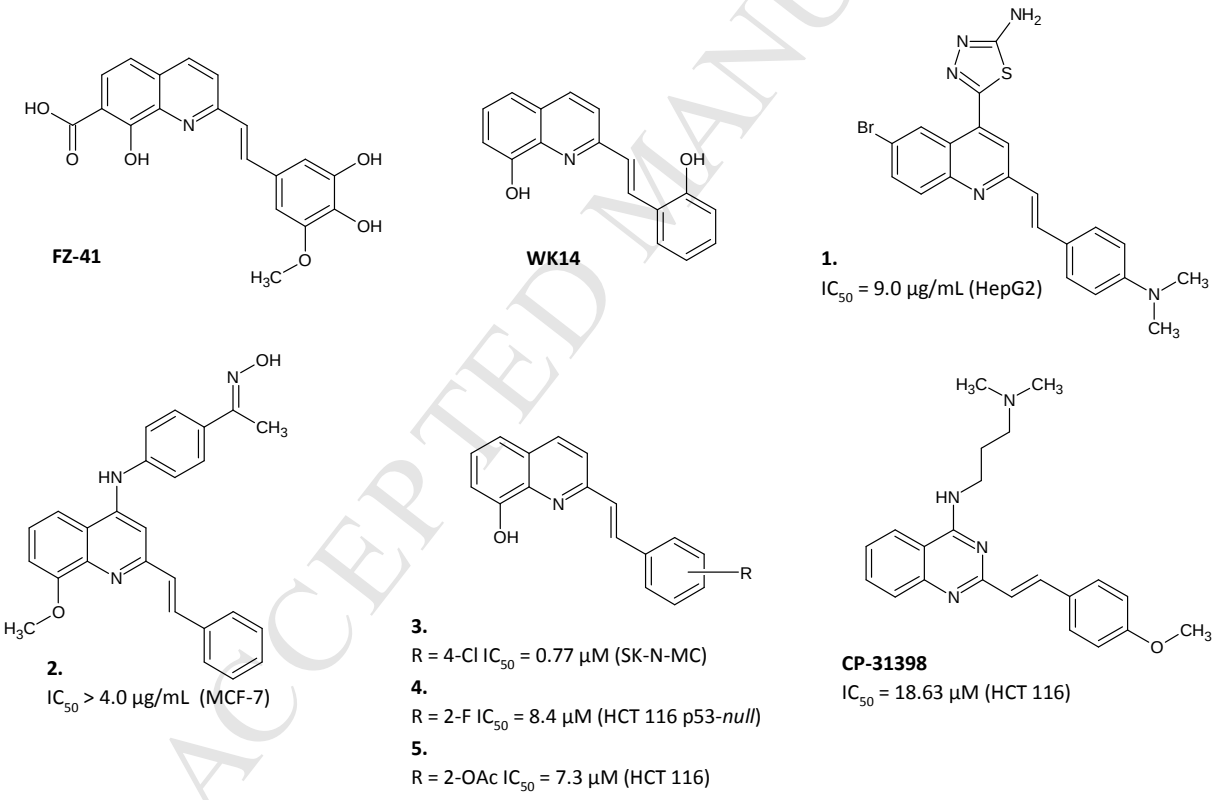

Fig. 1. Styrylquinoline as versatile scaffold for anticancer activity.

SQ that had been substituted with thiadiazole at the C4 position of quinoline (**1** in **Fig. 1.**) appeared to be active against liver cancer cell lines (HepG2) [16]. Moreover, it was found to be an active inhibitor of EGFR kinase with a potency that was similar to sorafenib. Other SQ that had been designed on 4-chloro or 4-phenylamino quinoline were described by Chang *et*

al. [17]. These compounds (**2** in **Fig. 1.**) were also characterized by a good submicromolar activity level against breast cancer line (MCF-7). The authors postulated that the SQ block the cell cycle at the S phase and induce apoptosis. These facts along with their larger, aromatic structure may suggest a DNA intercalation. Unfortunately, their selectivity toward normal cells was not tested. However, in another report concerning furanyl analogs, the active compounds appeared to have a rather low selectivity [18]. A significant increase in their activity level and selectivity has been observed for derivatives of 8-hydroxyquinoline. A series of such derivatives that were halogenated in the styryl ring (**3**-**5**) had a superior activity along with good selectivity indexes compared to the unsubstituted SQ [19]. Oxine (8-hydroxyquinoline) is a known chelating agent and many compounds with this fragment exert their biological activity through interactions with metal cations. Oxine itself is broadly used as antibacterial, antifungal and antiparasitic agent in various applications. For these SQ, the molecular mechanism of activity was established based on the strong correlation of the activity with lipophilicity and the intercellular localization of the drug. Apparently, SQ penetrates the mitochondrial membrane and causes leakage of the cytochrome c followed by the activation of the caspase apoptosis pathway. A similar mechanism, which consists of disrupting the mitochondrial functionality was proposed earlier for amine substituted SQ [20]. What is even more appealing is that the dihalogenated compounds (e.g. **4** in **Fig. 1.**) were found to be considerably more active against colon cancer that had a deletion of *TP53* tumor suppressor gene. Mutations in the *TP53* gene can be found in half of the cancers that are diagnosed and are often considered to be a sign of drug resistance and a poor prognosis. Typical cytostatic drugs are often less effective against cancer lines that have such mutations. With this in mind, a high activity against p53-*null* cells combined with a good selectivity is particularly appealing. Another compound, CP-31398, which is a quinazoline analog of SQ (**Fig. 1.**), should also be mentioned in relation to p53. This styrylquinazoline is known to be a reactivator of a misfolded mutant protein [21]. Although its mechanism of action is not clear, it may stabilize the protein in the correct spatial (DNA-binding) form, thereby promoting its proapoptotic activity. Although it was designed for mutants with a point mutation, it is also active in the wild-type cells [22][23]. More recently, a similarity between CP-31398 and kinase inhibitors has been exploited in the design of novel styrylquinazoline anticancer agents [24].

Unfortunately, in some mutants, and particularly in cells that have more damage in the genome (e.g. as a deletion), the reactivator appeared to be ineffective. Actually, compared to

the wild-type and p53-*null* colon adenocarcinoma, the CP-31398 was found to be inactive in concentrations that are cytotoxic to normal cells [19,24]. Thus, SQ that are equally potent against the wild-type and mutant as well as p53-*null* cells are a promising class of compounds that deserve further exploration. Unfortunately, there are some serious gaps in our knowledge on SAR as only several compounds with a good activity level have been described to date. Therefore, in our current work we plan to perform a more in-depth analysis of the structural factors that determine the activity level. We designed a series of SQ from 8-hydroxyquinoline and its 5,7-dichloroderivative as they are the most promising among those that have been described in the literature [25][7]. Another scaffold that was reported is 4-substituted quinoline, e.g. 4-hydroxy or 4-phenyl [17]. On the other hand we used various substituents in the styryl part of the molecule in order to cover a relatively broad range of electronic effects.

2. Results and discussion

2.1. Chemistry

All of the compounds that were studied were synthesized from the commercially available quinaldines A-D. The first step of this synthesis consisted of condensing the appropriate aromatic aldehyde using the conventional or microwave heating methods (MAOS)[26] according to **Scheme 1**. The conventional reactions were performed in a mixture of boiling acetic anhydride and acetic acid. The result of such a selection of conditions is the acylation of the hydroxyl groups of the reactants. Accordingly, the next step was the hydrolysis of the resulting reaction of the acyl group(s). These groups were selectively removed with pyridine/water or K_2CO_3/methanol mixtures as was previously described [19].

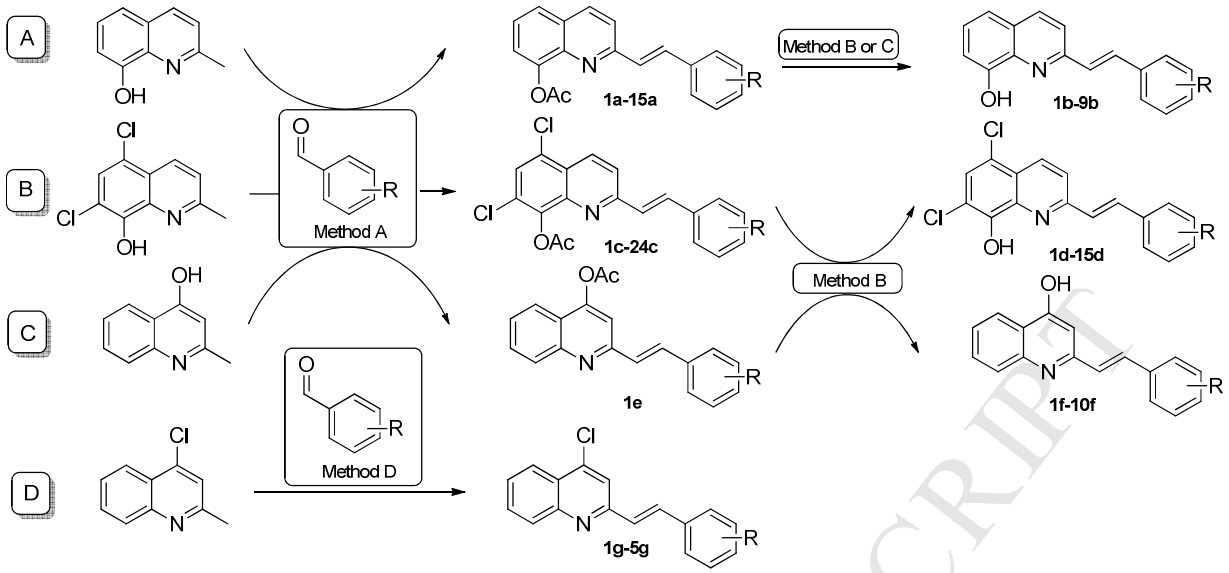

Scheme 1. Synthesis of the compounds that were studied.

2.2. Biological studies

2.2.1. Antiproliferative assay

The anti-proliferative activity of the synthesized compounds was tested against the human colon carcinoma cell lines, the wild type (HCT 116 $p53^{+/+}$) and p53 negative (HCT 116 $p53^{-/-}$) with an MTS assay. Additionally, the compounds were also tested for their cytotoxicity against normal cells – human fibroblasts (NHDF). The results related to the antiproliferative activity assays are shown in **Table 1**.

Table 1. Anti-cancer activity of the compounds that were studied (ND – not determined).

Group	No.	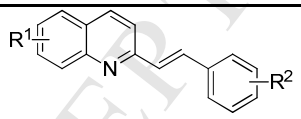		IC_{50} [μM]		
		R^1	**R^2**	**HCT 116 $p53^{+/+}$**	**HCT 116 $p53^{-/-}$**	**NHDF**
A	**1a**	8-OAc	2-OCH_3	13.13 ± 1.98	13.44 ± 1.39	>25
	2a		3-OCH_3	**9.70 ± 0.46**	10.35 ± 0.84	>25
	3a		4-OCH_3	11.65 ± 0.73	11.16 ± 1.13	>25
	4a		3,4-OCH_3	16.84 ± 0.44	14.74 ± 0.56	> 25
	5a		3,5-OCH_3	>25	>25	ND
	6a		2-OEt	20.26 ± 4.44	19.76 ± 1.16	>25
	7a		4-OEt	20.87 ± 0.84	15.48 ± 1.42	>25
	8a		3-OAc	**5.40 ± 0.37**	**4.82 ± 0.66**	> 25
	9a		4-OAc	>25	>25	ND
	10a		2-Cl	10.63 ± 0.41	**8.86 ± 0.83**	>25
	11a		3-Cl	14.47 ± 0.68	10.87 ± 1.71	>25
	12a		2,3-Cl	>25	**9.38 ± 0.87**	>25
	13a		2,6-Cl	>25	>25	ND

	14a		2- NO_2	**4.60 ± 0.22**	**4.54 ± 0.31**	>25
	15a		2,4-NO_2	>25	>25	ND
	1b		4- OCH_3	>25	>25	ND
	2b		3,5-OCH_3	>25	19.28 ± 1.15	>25
	3b		4-OH	13.53 ± 1.76	16.61 ± 1.59	>25
	4b		2-OAc	**7.32 ± 1.01**	13.53 ± 0.81	**6.92 ±1.72**
	5b	8-OH	4-OAc	12.36 ± 0.91	15.48 ± 1.84	>25
	6b		2-Ac-4Cl	19.92 ± 0.50	18.61 ± 1.23	>25
	7b		2,6-Cl	>25	>25	ND
	8b		2-Cl-6-F	>25	>25	ND
	9b		2-NO_2	11.72 ± 0.45	**2.61 ± 0.35**	>25
B	**1c**		2-OAc	11.20 ± 0.47	**8.77 ± 1.44**	>25
	2c		2-OAc-5-Cl	13.85 ± 0.59	11.46 ± 0.50	>25
	3c		2-OAc-3,5-Cl	**3.65 ± 0.22**	**4.72 ± 0.26**	13.83 ± 0.46
	4c		2-OAc-3-Br-5-Cl	**3.83 ± 0.14**	**4.39 ± 0.23**	13.36 ± 0.64
	5c		2-OAc-3,5-I	**5.13 ± 0.27**	**3.90 ± 0.16**	13.09 ± 0.75
	6c		2-I	**1.20 ± 0.16**	**2.40 ± 0.56**	15.39 ± 0.74
	7c		2-Cl	**2.22 ± 0.27**	**1.30 ± 0.13**	>25
	8c		2,6-Cl	**5.93 ± 0.70**	**6.06 ± 0.96**	**9.55 ± 1.58**
	9c		2-Cl-6-F	**3.41 ± 0.36**	**2.73 ± 0.37**	23.46 ± 1.44
	10c		2-Br-6-F	**3.70 ± 0.38**	**2.90 ± 0.28**	>25
	11c		2,5-F	**2.57 ± 0.37**	**4.47 ± 1.00**	20.38 ± 0.89
	12c		2,6-F	**4.93 ± 0.25**	**4.49 ± 0.51**	>25
	13c	5,7-Cl-8-OAc	2,6-F-3-Cl	**7.26 ± 0.36**	**4.82 ± 0.52**	21.38 ± 2.21
	14c		2,6-F-4-Cl	20.90 ± 0.71	12.15 ± 1.86	>25
	15c		2-CN	**0.93 ± 0.12**	**1.08 ± 0.11**	>25
	16c		3-CN	**1.39 ± 0.18**	**1.47 ± 0.50**	11.15 ± 2.53
	17c		4-CN	**1.78 ± 0.53**	**1.92 ± 0.19**	20.00 ± 1.04
	18c		2-OAc-3-NO_2	**2.71 ± 0.16**	**2.61 ± 0.33**	20.23 ± 1.27
	19c		2-OAc-5-NO_2	**4.76 ± 0.47**	**3.60 ± 0.70**	22.16 ± 0.77
	20c		3-NO_2-4-OAc	**4.22 ± 0.32**	**4.52 ± 0.16**	>25
	21c		2-NO_2	**0.85 ± 0.11**	**0.78 ± 0.13**	22.29 ± 1.01
	22c		3- NO_2	**1.74 ± 0.10**	**1.01 ± 0.07**	11.09 ± 0.35
	23c		4- NO_2	**2.31 ± 0.30**	**2.01 ± 0.53**	19.94 ± 1.98
	24c		2,4-NO2	**0.28 ± 0.04**	**0.27 ± 0.03**	14.59 ± 0.81
	1d		2-OH	10.48 ± 2.14	15.30 ± 1.84	>25
	2d		2-OAc-3,5-Cl	**4.09 ± 0.28**	**4.03 ± 0.34**	16.99 ± 1.58
	3d		2-OH-3-Br-5-Cl	**3.28 ± 0.42**	**2.58 ± 0.25**	14.65 ± 0.99
	4d		2-Cl	**1.88 ± 0.85**	**2.86 ± 1.00**	12.57 ± 2.88
	5d		2,3-Cl	**5.27 ± 1.02**	**4.00 ± 0.37**	**4.50 ± 0.27**
	6d		2-Cl-6-F	**7.30 ± 1.02**	**4.50 ± 1.10**	>25
	7d		2-I	**3.29 ± 0.38**	**1.85 ± 0.56**	>25
	8d	5,7-Cl-8-OH	2-CN	**0.86 ± 0.07**	**0.58 ± 0.08**	>25
	9d		3-CN	**8.51 ± 0.77**	**5.28 ± 1.20**	17.40 ± 0.85
	10d		4-CN	**3.10 ± 0.04**	**2.46 ± 0.34**	**7.97 ± 0.55**
	11d		3-NO_2-4-OAc	**3.63 ± 0.14**	**3.28 ± 0.69**	22.78 ± 0.97
	12d		2-NO_2	**0.73 ± 0.12**	**0.54 ± 0.17**	>25
	13d		3-NO_2	**2.77 ± 0.54**	**1.03 ± 0.32**	**9.82 ± 1.10**

	14d		4-NO_2	**6.48 ± 0.42**	**3.39 ± 0.35**	>25
	15d		2,4-NO2	**0.75 ± 0.30**	**0.76 ± 0.16**	>25
C	**1e**	4-OAc	2-I	>25	>25	ND
	1f	4-OH	2-OAc	>25	>25	ND
	2f		4-OAc	>25	>25	ND
	3f		2-I	>25	>25	ND
	4f		2-Cl	>25	>25	ND
	5f		3-Cl	>25	>25	ND
	6f		2,3-Cl	>25	>25	ND
	7f		2-CN	>25	>25	ND
	8f		3- NO_2	>25	>25	ND
	9f		4-NO_2	>25	>25	ND
	10f		2,4-NO_2	>25	>25	ND
D	**1g**	4-Cl	4-CN	>25	>25	ND
	2g		2-NO_2	>25	>25	ND
	3g		3-NO_2	>25	>25	ND
	4g		4-NO_2	>25	>25	ND
	5g		2,4-NO_2	>25	>25	ND
CP-31398			-	18.63 ± 0.92	26.28 ± 1.41	12.26 ± 0.54
5-Fluorouracil			-	**4.42 ± 0.70**	**4.69 ± 0.33**	>25
Doxorubicin			-	**0.34 ± 0.04**	**0.38 ± 0.03**	**0.14 ± 0.03**

During the analysis of the structure-activity relationship, the effect of the quinoline substituents as well as the phenyl ring on antitumor activity was observed. IC_{50} values below 1 are highlighted in red and those in the 1-10 range are bolded for better readability. All of the compounds could be divided into four groups (A, B, C and D) according to their structural scaffolds (**Scheme 1**). The biological activity results are consistent with this division. In general, the styrylquinolines that were based on quinoline substituted at the C-4 position (C and D groups) were inactive. Compounds that were based on 8-hydroxyquinoline or 8-acyloxyquinoline (group A) were moderately active, while their analogs that were designed on chloroquine (dichloro derivatives – group B) were the most active in this series. It seems that the modulation of nitrogen pKa is not crucial factor. The quinolines that were unable to chelate metal ions (unsubstituted at C-8 position) generally lacked any antitumor activity. These results are in good agreement with our previous work [19]. The importance of the hydroxy or acyloxy group at the C-8 position for antitumor activity suggest that metal chelation is a relevant mechanism of this activity [27,28]. In most cases, a quinoline substitution with an acyloxy group resulted in a better antitumor activity than a substitution with a hydroxy group (compare: **14a**/**9b**, **22c**/**13d**, **16c**/**9d**, **24c**/**15d**, etc.). The exceptions to this rule were very few and they were basically within the measurement error (compare: **21c**/**12d**, **20c**/**11d** and **15c**/**8d**). This observation is an important clue for understanding the possible mechanism of action. An obvious change in lipophilicity or solubility and an effect

on pharmacodynamics is not the case in the conditions of *in vitro* tests that are performed on cellular cultures. On the other hand, both 8-hydroxyquinoline and its acetylated derivative are known for their ability to chelate metal cations. However, the 2-methyl derivative has higher pKa of conjugate acid than its parent acetylated oxine. Moreover, in the presence of Cu^{2+} ions, the hydrolysis of the acetoxy group is more rapid and is the first order in attacking the hydroxyl group [29]. This, in turn, may improve the redox strength of the resulting complex, thereby allowing it to participate in the Fenton reaction and in the production of the hydroxyl radical and other reactive oxygen species (ROS) [30]. Another clear trend in the substitution pattern can be observed in the phenyl ring of the styryl group. The stronger effect of the electron-withdrawing group; the higher the antitumor activity. Namely, it turns out that a substitution of the phenyl ring at the 2-position affects the activity level of the individual derivatives in the order that is shown in the **Table 2** (entries 1 and 2). The derivatives with cyano and nitro substituents showed the highest activity level. The most active were the *ortho* derivatives followed by the *meta* and *para* derivatives, which were generally less active in each group (**Table 2**, entry 3). The introduction of a second nitro group into the phenyl ring increased the activity level even further and the 2,4-dinitro derivatives in group B were the most active against both of the cancer cell lines that were tested. The most active compound was **24c**, which reached a 0.27 μM level on HCT 116 $p53^{-/-}$ cell line. At the same time, it was favorably selective with the toxicity indexes that were higher than 55 (all of the selectivity indexes are listed in **Table S1** of the Supporting Information). As proof, the introduction of an electron-donating group (acyloxy group) into the phenyl ring with the nitro substituent reduced the activity level (compare: **22c** vs. **18c**, **19c**, **20c** and **13d** vs. **11d**). A striking exception among the 8-acyloxyquinoline derivatives was **15a**, which despite a 2,4-NO_2 substitution appeared to be inactive in our tests. This is even more surprising compared to **14a** (2-NO_2), which was the most active in this group of derivatives. When considering selectivity, it should be noted that the styrylquinolines from the B group were less selective toward normal fibroblasts. However, the majority of the active compounds that are presented in **Table 1** had a reasonable selectivity index within a range of 5-10. In general, the *meta*-substituted compounds with the electron-withdrawing group were less selective (compare: **16c** vs. **15c**, **17c**; **22c** vs. **21c**, **23c**; **13d** vs. **12d**, **14d**).

Table 2. The substitution pattern of the anticancer activity of styrylquinolines.

No.	Structure	Related anticancer activity
1.	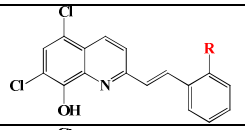	**2-OH** < **2-Cl/I** < **2-CN** < **2-NO_2**
2.	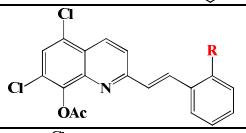	**2-OAc** < **2-Cl/I** < **2-CN** < **2-NO_2**
3.	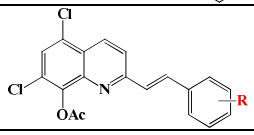	**4- NO_2 4-CN** < **3- NO_2 3-CN** < **2- NO_2 2-CN** < **2,4-NO_2**

Based on the first cytotoxicity screen on the HCT 116 cell line (**Table 1**), we selected a group of the most active compounds to be investigated further. In our previous studies, we were focused on the activity toward cell lines with a mutation in the *TP53* suppressor gene [19][31]. The p53 protein is an attractive target for anticancer studies because of its common mutations in malignant cells. As mentioned above more than half of all cancer cases have a mutation in the *TP53* gene, therefore, for our research we selected cell lines with a mutation (U-251, PANC-1) or deletion (double-deletion) in *TP53* (HCT 116 $p53^{-/-}$) or with total absence of *TP53* (AsPC-1) for further examinations. These six cell lines represent colon (HCT 116; $p53^{+/+}$ and $p53^{-/-}$) and pancreatic (PANC-1 and AsPC-1) cancers, which are some of the most common types of tumors. Additionally, we selected a glioblastoma (U-251) because of its aggressiveness, poor prognosis and difficulty in treatment. To determine the toxicity toward normal cells, we selected normal human dermal fibroblasts (NHDF).

The glioblastoma line U-251 carry a point missense mutation that results in a change of arginine into histidine at codon 273. The p53 protein for its regulatory function is important for ROS-related activity. The *TP53*-induced glycolysis and apoptosis regulator (TIGAR) is another regulatory protein that changes the cellular response to redox stress and damage. It has often been found to be overexpressed in gliomas [32]. The PANC-1 cell line has also been reported to have missense point mutations in 273 (Arg-His or Arg-Cys) [33]. However, according to the source, different positions and types of mutations have also been reported for these pancreatic cell lines [34,35]. Although p53 is typically considered to be the “guardian of the genome”, its mutation does not cause a loss of function or increase in the subsequent mutations. Because this protein is an important node between many pathways and also acts as gene regulator, it is not possible to predict the behavior of mutated p53 in cancer cells [36,37]. Consequently, some mutations are of the gain-of-function type as was reported for this

R273H in U-251 cells [38]. Through new interactions with other genes, the mutant p53 may acquire an oncogenic function.

In order to determine the expression of *TP53* in the cell lines that were tested, we performed a qRT-PCR analysis (**Fig. 2.**). The highest *TP53* expression was observed for HCT 116 $p53^{+/+}$ and subsequently for PANC-1.

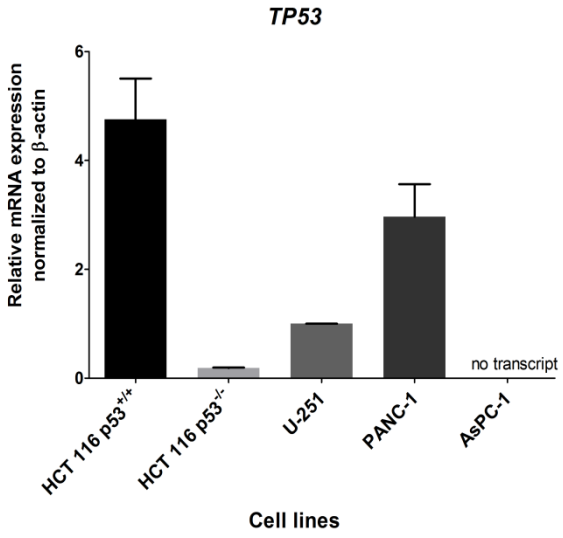

Fig. 2. mRNA expression of *TP53* in a panel of cancer cell lines. The results are shown as the mean ± SD of three independent measurements, each in triplicate.

As is presented in **Table 3**, all of the compounds that were tested were characterized by a good activity level against all of the cancer cell lines as well as selectivity toward normal cells. The IC_{50} parameter for cancer cells varied from 0.12 µM (compound **15d** on U-251) to 11.65 µM (compound **14d** on AsPC-1). In general, no significant differences were observed between the HCT 116 wild type ($p53^{+/+}$) and HCT 116 $p53^{-/-}$. However, the cytotoxicity of the compounds that were tested toward AsPC-1 had the lowest level, i.e. the compounds were significantly less active. For the rest of the cell lines that were tested, major differences in IC_{50} values were observed. The compounds that were investigated had rather similar levels of activity, except for the AsPC-1 cell line for which they had a low specificity. The activity level against fibroblasts was to determine the selectivity indexes (SI) of each cell line (**Table S1** in the **Supporting Information**).

Table 3. Cytotoxicity of the selected compounds that were studied on a panel of cell lines.

Compound	R^2	IC_{50} [μM]					
		HCT 116 $p53^{+/+}$	HCT 116 $p53^{-/-}$	PANC-1	AsPC-1	U-251	NHDF
7c	**2-Cl**	**2.22 ± 0.27**	**1.30 ± 0.13**	**2.14 ± 0.28**	**6.07 ± 0.68**	**5.70 ± 1.09**	>25
17c	**4-CN**	**1.78 ± 0.53**	**1.92 ± 0.19**	**1.82 ± 0.09**	**4.58 ± 0.74**	**3.67 ± 0.30**	20.00 ± 1.04
18c	**2-AcO-3-NO_2**	**2.71 ± 0.16**	**2.61 ± 0.33**	**6.16 ± 0.54**	10.91 ± 0.92	**5.11 ± 0.24**	20.23 ± 1.27
21c	**2-NO_2**	**0.85 ± 0.11**	**0.78 ± 0.13**	**2.51 ± 0.09**	**4.97 ± 0.32**	**2.30 ± 0.25**	22.29 ± 1.01
22c	**3-NO_2**	**1.74 ± 0.10**	**1.01 ± 0.07**	**2.30 ± 0.09**	**6.34 ± 0.36**	**3.07 ± 0.25**	11.09 ± 0.35
24c	**2,4-NO_2**	**0.28 ± 0.04**	**0.26 ± 0.03**	**0.57 ± 0.06**	**5.30 ± 0.14**	**0.35 ± 0.05**	14.59 ± 0.81
8d	**2-CN**	**0.86 ± 0.07**	**0.58 ± 0.08**	**3.39 ± 0.42**	**7.81 ± 0.84**	**3.08 ± 0.53**	>25
12d	**2-NO_2**	**0.73 ± 0.12**	**0.53 ± 0.17**	**0.89 ± 0.07**	**7.41 ± 0.78**	**2.04 ± 0.42**	>25
14d	**4-NO_2**	**6.48 ± 0.42**	**3.39 ± 0.35**	**8.25 ± 1.20**	11.65 ± 1.04	**8.78 ± 0.84**	>25
15d	**2,4-NO_2**	**0.75 ± 0.30**	**0.76 ± 0.16**	**0.49 ± 0.08**	**1.67 ± 0.17**	**0.12 ± 0.02**	>25
CP-31398	**-**	18.63 ± 0.92	26.28 ± 1.41	>25	ND	18.77 ± 1.65	12.26 ± 0.54
Doxorubicin	**-**	**0.34 ± 0.04**	**0.38 ± 0.03**	**0.730 ± 0.088**	**0.86 ± 0.13**	**0.05 ± 0.01**	**0.14 ± 0.03**

2.2.2. Cell Cycle

The promising activity profiles against the cancer cell lines prompted us to run further experiments. We hypothesized that the compounds that were tested could affect the inhibition of the cell cycle, while the lack of any significant differences between the IC_{50} values for both HCT 116 cell lines ($p53^{+/+}$ and $p53^{-/-}$) suggest a p53-independent mechanism of action. However, some resistance was observed for the AsPC-1 cell line. Therefore, we decided to explore the effect of the selected compounds, **12d** and **24c**, on the progression of the cell cycle in the HCT 116 $p53^{+/+}$ and U-251 cell lines that had been selected as the wild type and a partially functional mutant of p53. The results of these experiments are presented in **Fig. 3**. After incubation with the tested compounds, no significant differences were observed in the G0/G1 phases for the controls and treated cells, but a negligible decreasing trend was

noticeable. The reverse occurred for the S phase, which was increased; however, significant growth was detected for HCT 116 $p53^{+/+}$. These observations suggest that the compounds that were tested inhibit the cell cycle in the S phase.

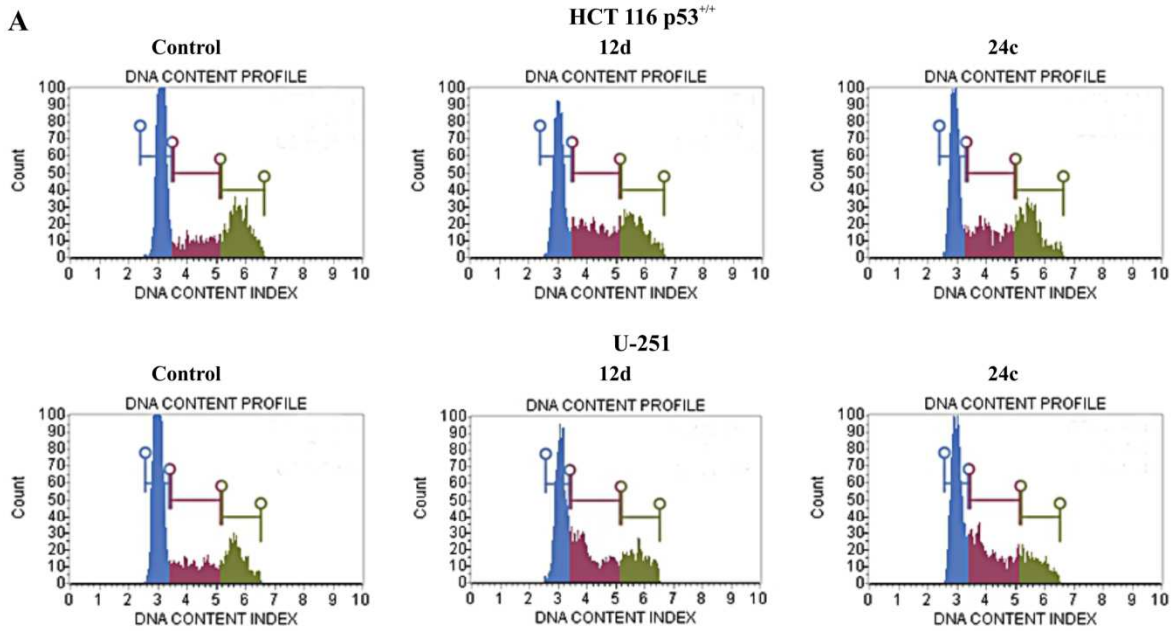

B

	HCT 116 $p53^{+/+}$			U-251		
	Control	**12d**	**24c**	**Control**	**12d**	**24c**
G0/G1 [%]	56.03 ± 7.72	45.2 ± 3.47	45.2 ± 4.33	50.93 ± 7.31	47.6 ± 6.44	44.67 ± 3.04
S [%]	14.3 ± 2.15	25.93 ± 1.42	26.37 ± 2.07	16.27 ± 1.46	20.13 ± 4.23	24.17 ± 3.35
G2/M [%]	23.1 ± 4.94	19.77 ± 3.76	19.13 ± 3.95	18.7 ± 0.2	18.9 ± 3.46	17.93 ± 1.00

C

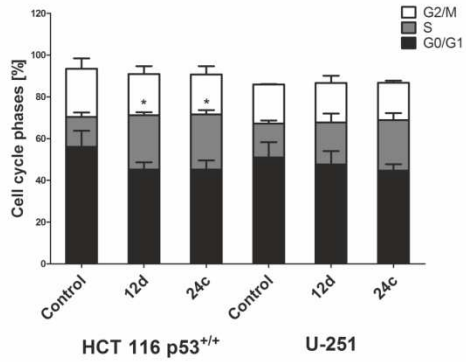

Fig. 3. Effect of the treatment with styrylquinolines (10xIC_{50}) on the cell cycle in the HCT 116 $p53^{+/+}$ and U-251 cells. (A) Representative histograms from one of three independent experiments showing the distribution of cells in the individual phases of the cell cycle. (B) Table with the mean ± SD percentage of the cells in the individual phases of the cell cycle from three independent experiments. (C) Diagram of the data with statistical analysis using a one-way ANOVA with Bonferroni's post-hoc test: *p < 0.05, **p < 0.01, ***p < 0.001 compared to the respective control.

2.2.3. Annexin V Binding

The type of cell death was another factor in determining the potential mechanism of action for SQ. The assay was based on measuring the FITC fluorescence, that was conjugated

to Annexin V, in the apoptotic cells. Annexin V is a cellular protein that binds to phosphatidylserine – an indicator of apoptosis. A damaged cell loses the integrity of the cell membrane and phosphatidylserine is moved outside the cell, which results in the emission of a green signal of the FITC and indicates apoptotic cell death. For this experiment, we selected the same two cell lines – HCT 116 $p53^{+/+}$ and U-251. Incubation with **12d** and **24c** enabled the following conclusions to be drawn. While an apoptotic cells fraction was observed for both derivatives, the strongest effect was detected for **24c** for HCT 116 $p53^{+/+}$ (63.10% of the apoptotic; **Fig. 4B**). This increase in the apoptotic cells was also observed in the U-251 cells but to a lesser extent.

A

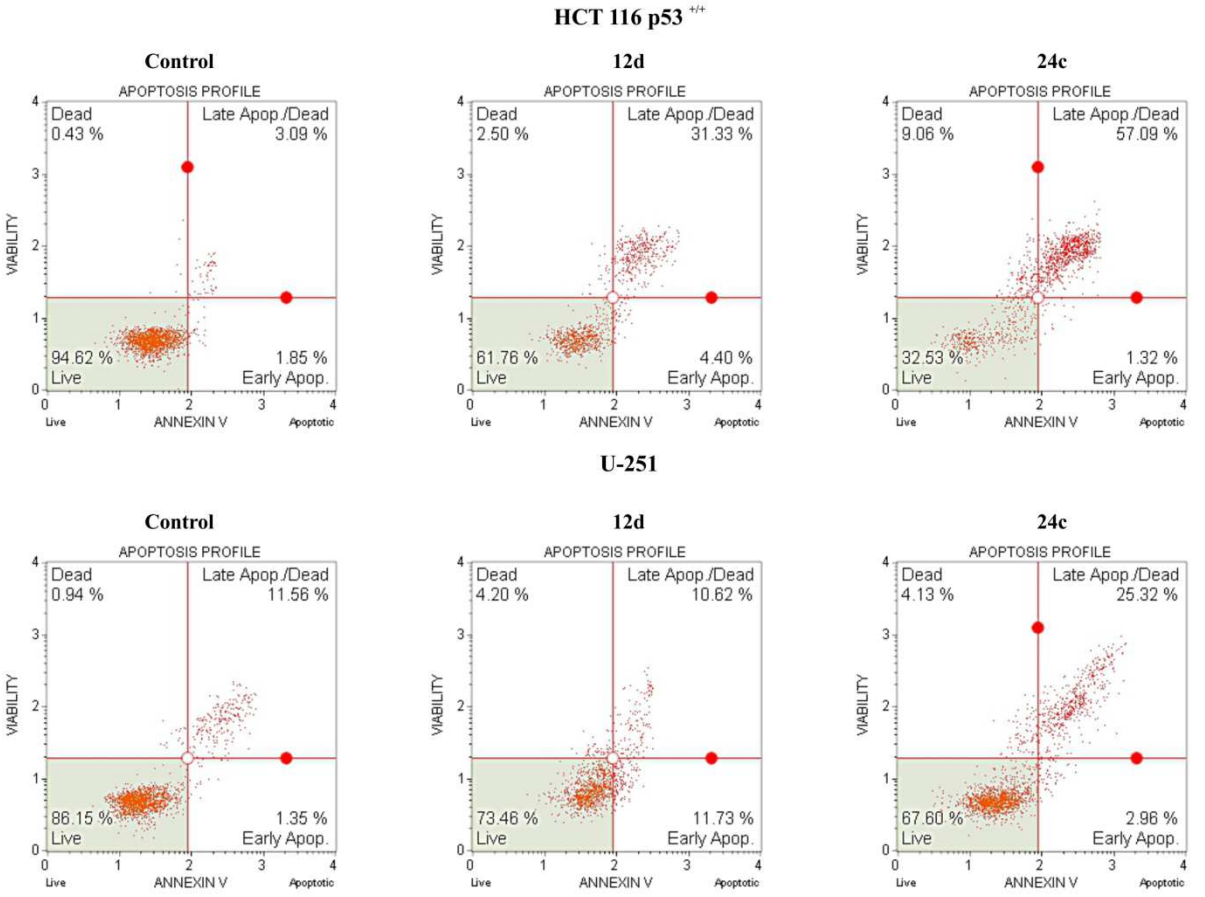

B

	HCT 116 p53$^{+/+}$			U-251		
	Control	**12d**	**24c**	**Control**	**12d**	**24c**
Live	95.88 ± 1.08	65.42 ± 8.86	35.79 ± 4.04	89.75 ± 2.3	76.04 ± 4.16	68.03 ± 1.54
Total apoptotic	3.99 ± 1.21	33.78 ± 8.78	63.1 ± 3.92	10.11 ± 2.56	23.67 ± 4.97	32.31 ± 7.12

C

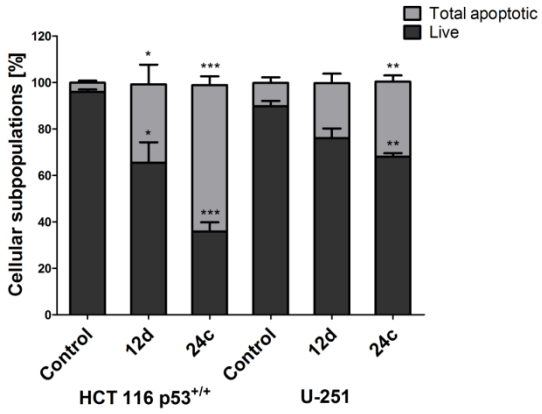

Fig. 4. Evaluation of the affect of the treatment with styrylquinoline analogs (20 µM) on the induction of apoptosis in the HCT 116 p53$^{+/+}$ and U-251 cells after 48h. (A) Representative histograms from one of three independent experiments show the percentage of live, early and late apoptotic cells. (B) Table shows the mean ± SD percentage of live and total apoptotic cells from three independent experiments. (C) Diagram of the data with a statistical analysis using a one-way ANOVA with Bonferroni's post-hoc test: *p < 0.05, **p < 0.01, ***p < 0.001 compared to the respective control.

2.2.4. ROS generation

As was mentioned above, chelating the metal cations that are redox active (such as copper and iron) may lead to the formation of reactive oxygen species and cause oxidative damage. In larger aromatic structures such as SQ, the same can be associated with DNA intercalation, which results in minor, cumulative damage in a genome. This, in turn, leads to an arrest of the cell cycle and apoptosis in proliferating cells. Our previous works [39][40][41] promted us to examite the affect of the compounds that were tested on the generation of ROS. For this purpose, we conducted a series of the experiments that involved the incubation of the selected derivatives **12d** and **24c** with the HCT 116 $p53^{+/+}$ and U-251 cell lines after which the ROS level was measured using a fluorescent assay.

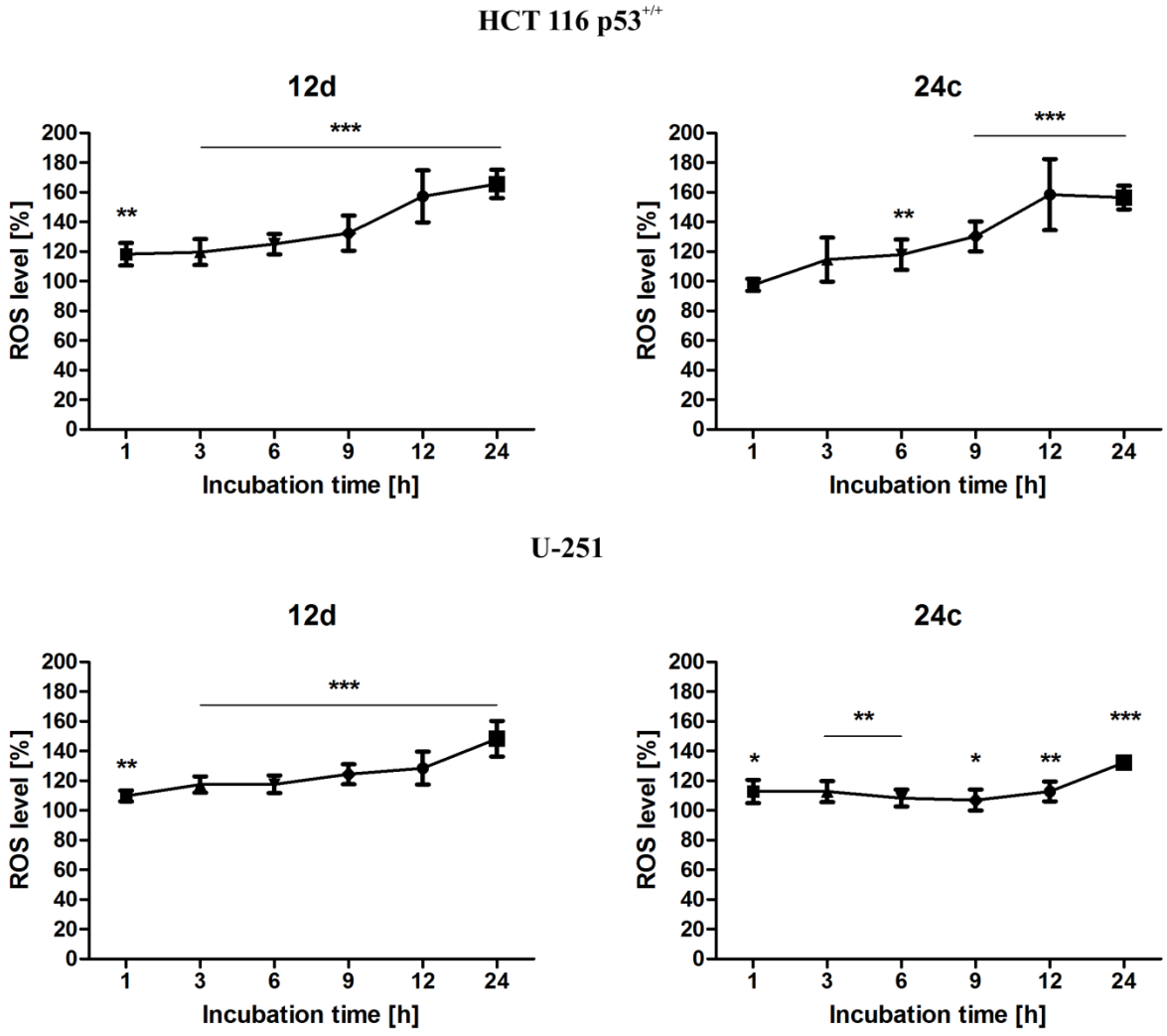

Fig. 5. Impact of the compounds that were tested (20 µM) on the generation of ROS in the HCT 116 $p53^{+/+}$ and U-251 cells. Data were normalized to control (untreated cells). Results are presented as the mean ± SD of three independent measurements. Data were

analyzed using the Student's t-test: *p < 0.05, **p < 0.01, ***p < 0.001 compared to the control group.

The results presented in **Fig. 5** indicated that ROS were generated by both of the compounds that were tested on both cell lines. We performed kinetic measurements in the time range of 1-24h, which indicated an increasing trend in all cases. The largest increase of the ROS level was observed for HCT 116 $p53^{+/+}$ (over 160%). The highest ROS concentration was detected after 24h and was still increased. The level of ROS and their function of signaling factors is closely correlated with the activity of p53 [42]. p53 has a downregulating effect on MnSOD – one of the main proteins that constitutes an antioxidant defense of a cell. The loss of the p53 function, which is caused by a mutation, may lead to higher antioxidative potential in cancer cells [43,44]. The same can be observed in our results in which the generation of ROS was higher in the wild-type cells.

2.2.5. Western Blot

After previous analyses, we had no doubt that the styrylquinoline derivatives that were being examined affected the regulation of the cell cycle and the induction of apoptosis. In order to confirm the inhibition of the cell cycle and apoptosis induction that were observed and to investigate the mechanism of action of the compounds that were tested more deeply, we performed a western blot analysis. Additionally, after the kinetic determination of the intracellular ROS levels, we decided to examine the expression of the oxidative stress-related proteins. A visualization of the protein bands with their corresponding densitometric analysis is presented in **Fig. 6**.

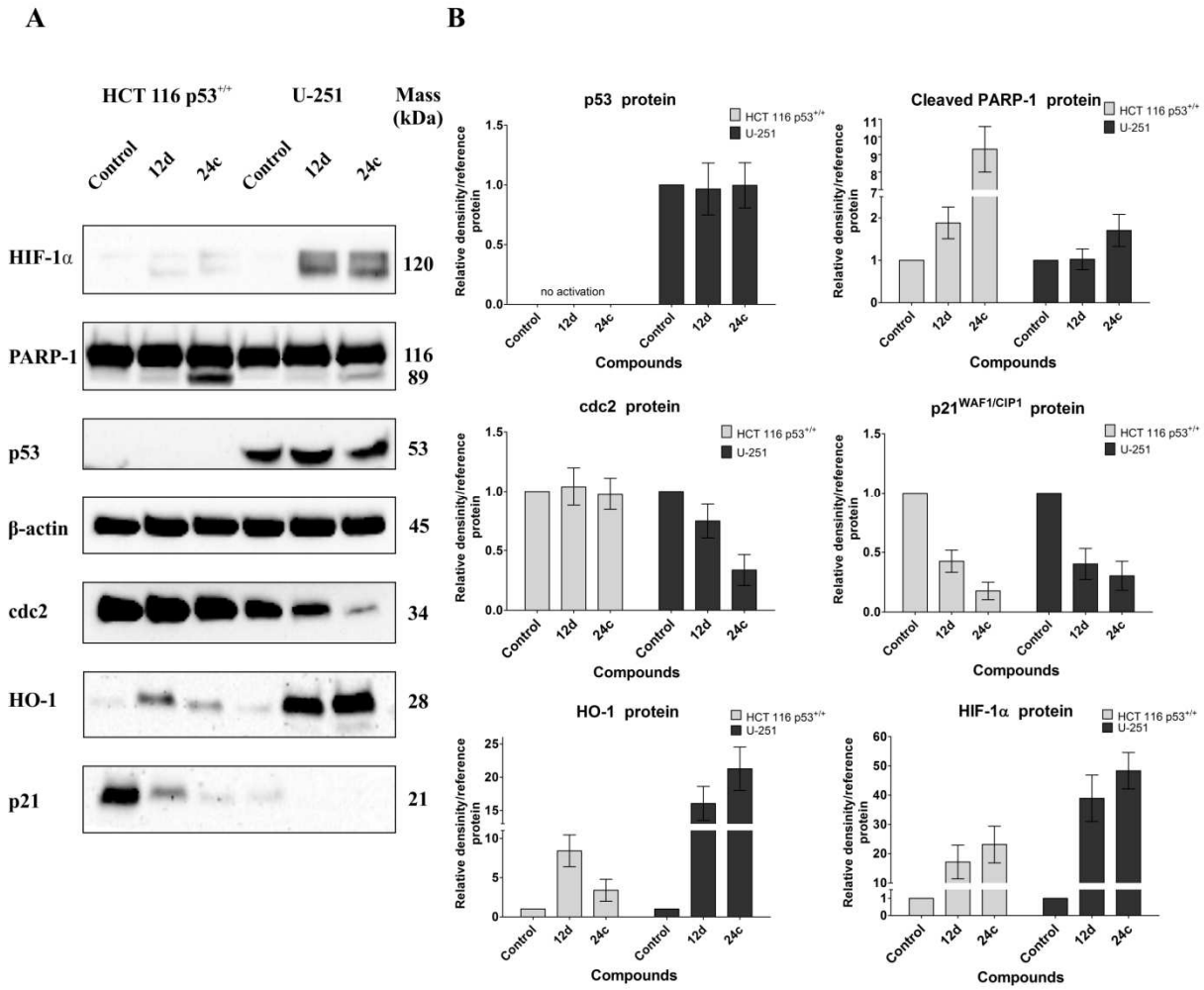

Fig. 6. Effect of the styrylquinoline analogs (20 μM) that were tested on the expression of HIF-1α. PARP-1, p53, β-actin, cdc2, HO-1, p21 in the HCT 116 p53$^{+/+}$ and U-251 cells. (B) Densitometric analysis of the data that was obtained normalized to the reference proteins are shown as the mean ± SD of four independent experiments.

A cytotoxicity analysis on the cell lines for various *TP53* gene expressions indicated that there was no correlation between the activity of the compounds that were tested and p53 activation. Indeed, in the western blot analysis, no effect of the tested **12d** and **24c** derivatives on the activation of the p53 protein was observed. Although p53 was activated at a certain level in U-251, there were no differences between the control cells and the cells after treatment with the compounds that were investigated. The expression of this protein in U-251 is most likely related to a mutation at position 273 [38]. A similar level of p53 in this cancer cell line was observed in a study of the menavolate pathway in glioblastomas [45]. Our results clearly indicated a p53-independent mechanism of action of the styrylquinoline analogs and confirmed our previous work on this group of compounds [19].

One of the important enzymes that are associated with the apoptosis pathway is Poly (ADP-rybose) polymerase-1 (PARP-1), which is the target of caspases. The main role of this protein is to support the cells viability by its involvement in the repair of the DNA damage that is triggered by stress factors. The degradation of PARP-1, which was observed as the cleavage by caspases, promoted the destabilization of cells. Cleaved PARP is considered to be a good indicator of apoptotic cells [46][47][48]. Clear cleavages were observed in both cell lines after treatment with the **24c** derivative. The most distinct cleavage was observed in HCT 116 ($p53^{+/+}$) and cleavage for **12d** was also detected for this cell line. Therefore, the result in this case strongly confirms the data that was obtained from the annexin V binding assay.

The compounds that were tested also contributed to the arrest of the cell cycle in the S phase in the case of HCT 116 ($p53^{+/+}$), and to a lesser extent in U-251. A lower level of the two proteins (cdc2 and p21), which are related to untreated cells, were observed in the glioblastoma cell line. Cyclin-dependent kinase 2 (cdc2) participates in the transition of cells from the G2 phase into the M phase [49]. On the other hand, $p21^{WAF1/CIP1}$ regulates the activity of cyclin and kinases during the progression of the cell cycle [50]. Downstream of $p21^{WAF1/CIP1}$, which inhibits the cell cycle in the S phase as well as significant increase population of the apoptotic cells, was also observed in keranocytes after an anti-proliferative factor was applied [51]. We suppose that in the U-251 cells, the derivatives that were tested may cause arrest in both the S and G2/M phases. Confirmation of our thesis was the downregulation of cdc2. In HCT 116 ($p53^{+/+}$), however, there were no significant differences between the cdc2 expression, which proved that the cell cycle had been inhibited in the earlier G1 phase. Additionally, a p53-independent mechanism of G1 inhibition was observed in HCT 116 in which an increase of $p21^{WAF1/CIP1}$ plays important role [52]. These results seem to be opposite to ours due to the decrease in the level of $p21^{WAF1/CIP1}$ and the arrest of the cell cycle in other phases. However, the factors that are involved in the mechanism of action of a specific drug depend on the cell line being tested, the dose of a drug, the time point being tested and many other factors. Considering the dual role of the p21 protein [53], results that were observed are not surprising although some more detailed research would be valuable to explain these mechanisms.

In pathophysiological conditions, one of the crucial enzymes that are involved in maintaining proper homeostasis is heme oxygenase-1 (HO-1). During normal states, the level of HO-1 in cells is quite low. In response to numerous factors that lead to oxidative stress, HO-1 is highly activated [54][55]. The significant increase of HO-1 after treatment with the compounds that were tested in both cell lines is most likely the result of excessive

intracellular generation of ROS. These results are in agreement with the literature data, which suggest a correlation between increased ROS levels and the intensified activation of HO-1 [56]. The increasing production of ROS by mitochondria may also play an important role in promoting the expression of hypoxia-inducible factor-1 (HIF-1). Although this transcription factor is mostly connected with tumorogenesis, angiogenesis in solid tumors and a generally poor prognosis for patients, its growth may be related to oxidative stress [57][58]. Liang *et al*. [59] proved a time-dependent relationship between the growth of both the HIF-1 and ROS levels. The results of our work, in addition to the expansion of the generation of ROS, showed a high activation of HIF-1α after treatment with both SQ. Because the overexpression of this protein is connected with an accumulation of mutations in the tumor suppressor genes such as p53 [60], we detected a higher level of HIF-1 in U-251 than in HCT 116 ($p53^{+/+}$). Furthermore, in studies on the osteosarcoma cancer cell lines, apoptosis was partially inhibited by upregulating the expression of HIF-1 [59]. In other words, HIF-1 is another element of the cellular antioxidative potential along with MnSOD and the small molecular redactors such as glutathione, which is predominantly upregulated in the p53-mutated cancer cell lines. Moreover, the response of the wild-type p53 to ROS strongly depends on their initial level. p53 may act as an anti- or pro-oxidative regulator to promote survival or apoptosis respective to the severity of the damage [61]. On the other hand, p53 mutants develop a higher antioxidative capacity in order to fulfill their metabolic demand on ROS, which leads to a more fragile equilibrium that can easily be broken by drugs that increase the ROS.

Based on all of the results that were obtained, we suggest that the anti-proliferative effect of styrylquinolines is correlated with the overproduction of intracellular ROS. In our research, the oxidative stress that was induced by the compounds that were tested clearly activated the ROS-related pathways, thus leading to apoptosis. Apoptotic death via an elevated level of ROS is the mechanism that has also been determined in other glioma cell lines [62][63].

3. Conclusions

A series of styrylquinolines with diversified substituents were designed and synthesized. Their activity against a panel of cancer cells was evaluated, which provided data that was suitable for some SAR analyses. According to these results, the importance of the hydroxyl group in position C8 of quinoline is confirmed. Apparently, it is its chelating properties that extend the activity of SQ. This was also confirmed by a time-dependent

generation of ROS in cells after their incubation with those active compounds. The same can explain the high activity level of the acetylated derivatives, which can be more active in generating the redox reactions with iron or copper ions. On the other hand, strong electron-withdrawing substituents in the styryl part of a molecule are crucial for a high activity level. In fully aromatic flat molecules such as styrylquinolines, these effects have some influence on the electron density in the 8-hydroxyquinoline fragment, thus further increasing their chelation properties. An investigation of the mechanism of action revealed that the active SQ are also able to induce p53-independent apoptosis in cells that have a mutation in the *TP53* gene or those that are p53-null (deletion). Thus, their activity is generally at a similar level regardless of the p53 status of the cells, which is especially promising from the point of view of further development.

4. Experimental

All of the reagents were purchased from Aldrich. A Kieselgel 60, 0.040-0.063 mm (Merck, Darmstadt, Germany) was used for the column chromatography. TLC experiments were performed on alumina-backed silica gel 40 F^{254} plates (Merck, Darmstadt, Germany). The plates were illuminated under UV (254 nm) and evaluated in iodine vapor. The melting points were determined on an Optimelt MPA-100 apparatus (SRS, Stanford CA). The purity of the final compounds was checked using HPLC. Detection wavelengths of 210 and 250 nm were chosen for detection. The purity of individual compounds was determined from the area peaks in the chromatogram of the sample solution. All ^{1}H and ^{13}C NMR spectra were recorded on a Bruker Avance III 400 MHz FT-NMR spectrometer (400 MHz for ^{1}H and 101/126 MHz for ^{13}C, Bruker Comp., Karlsruhe, Germany). Chemical shifts are reported in ppm (δ) using signal of the solvent (DMSO-d_6, CD_2Cl_2-d_2, $CDCl_3$-d_1) as the reference against the internal standard $Si(CH_3)_4$. Easily exchangeable signals were omitted when they were diffuse. Signals are designated as follows: s, singlet; br. s, broad singlet; d, doublet; dd, doublet of doublets; ddd, doublet of doublet of doublets; t, triplet; tt, triplet of triplets; td, triplet of doublets; q, quartet; m, multiplet. Mass spectra were measured using a LTQ Orbitrap Hybrid Mass Spectrometer (Thermo Electron Corporation, USA) with direct injection into an APCI source (400°C) in the positive mode.

4.1. Synthesis of compounds

General Method A: The appropriate quinoline derivative (2.5 mmol) in acetic anhydride with 80% acetic acid was thoroughly mixed with one equivalent aldehyde and heated in an inert gas atmosphere (N_2) for 18-22 h at 130 °C. Then, the mixture was evaporated to dryness and a solid was crystallized from ethanol, methanol or ethyl acetate.

General Method B: The crude product from step A was transferred to a mixture of pyridine and water at a ratio of 3:1 and further heated for 3 h at 100 °C. Then, the mixture was evaporated to dryness and a solid was crystallized from ethanol, methanol or ethyl acetate.

General Method C: The appropriate styrylquinoline derivative (2.5 mmol) in methanol was thoroughly mixed with 2.5 equivalent K_2CO_3 for 2 h at room temperature. Then, concentrated HCl was added and the resulting precipitate was filtered and washed with H_2O. The crude product was recrystallized from ethanol, methanol or ethyl acetate.

General Method D: The appropriate quinoline derivative (2.5 mmol) and respective benzaldehyde (7,5 mmol) in 1:3 ratio was heated in an oil-bath at 175-180 °C. After 30-45 min of heating, the mixture was cooled to room temperature and washed with hexane (2x15mL) to remove excess benzaldehyde. The residue was recrystallized from ethanol, methanol or ethyl acetate.

Physicochemical data with spectroscopic analyses for all compounds are given in **Supporting Information**.

4.2. Biological studies

For biological experiments brief description is provided. For more details please refer to Biological Studies in **Supporting information**.

4.2.1. Cell culture

The human colorectal carcinoma cell line HCT 116 with wild type of p53 ($p53^{+/+}$) were obtained from the ATCC. HCT 116 with deletion of *TP53* gene ($p53^{-/-}$) was kindly provided by prof. M. Rusin from Maria Sklodowska-Curie Memorial Cancer Center and Institute of Oncology in Gliwice, Poland. The glioblastoma cell line U-251, two pancreatic cancer cell lines (PANC-1 and AsPC-1) were purchased from Sigma-Aldrich (Germany) and normal human dermal fibroblast cell line (NHDF) from PromoCell. Cells were grown as monolayer cultures in $75cm^2$ flasks in appropriate medium according to typical procedures. Cells were cultured under standard conditions at 37° C in a humidified atmosphere at 5% CO_2. Additionally, all cell lines subjected to routine mycoplasma test to ensure that there was no contamination.

4.2.2. Cytotoxicity studies

The exponentially growing cells were seeded into 96-well plates and cultured under standard conditions at 37° C for 24 h. Then, medium was supplied by solutions with varying concentrations of tested derivatives and further incubated for 72 h. After treatment, media solutions were replaced in each well by 100 μL DMEM without phenol red and 20 μL of CellTiter 96® AQueous One Solution-MTS (Promega), incubated for short time and measured. The results as medium for at least three independent experiments, were estimated using GraphPad Prism 5 as IC_{50} values.

4.2.3. Analysis of the level mRNA expression of *TP53*.

The total RNA was isolated from each cancer cell line according to the TRIzol procedure (Ambion). Then reverse transcription was conducted with 5 μg of total RNA using a GoScript™ Reverse Transcriptase kit (Promega) and Oligo$(dT)_{23}$ Primers (Sigma). The Real-Time PCR in a 20 μL reaction volume was performed with a CTX96 Touch™ Real-Time PCR Detection System (Biorad). All primer pair sequences (see Supporting Information) were ordered in Sigma-Aldrich. The reaction was performed and data was analyzed based on a comparison of the expression of the target gene to a reference gene – *ACTB* (β-actin), using the $2^{-\Delta\Delta CT}$ method. The experiments were repeated at least three times.

4.2.4. Cell cycle assay

The cells were seeded in 3 cm Petri dishes at a density of $0.2 \cdot 10^6$ cells per dish and incubated under standard conditions for 24 h. Afterwards, the medium was replaced by freshly prepared solutions of the tested styrylquinoline derivatives in tenfold IC_{50} values. After 24h, assays were performed using a Muse Cell-Cycle Kit (Millipore) in keeping with the manufacturer's instructions. Samples were incubated for 30 min at room temperature in the dark. After staining, the values of cellular subpopulations in individual cell cycle phases were assessed. The experiments were repeated at least three times.

4.2.5. Annexin V binding assay

The FITC Annexin V Apoptosis Detection KIT with 7-AAD (BioLegend) was performed according to manufacturer's instructions. The cancer cells were incubated on Petri dishes with medium solutions of tested styrylquinoline analogues (20 μM) for 48 h. After then, the cells were detached and centrifuged at 300 g for 5 min, then washed twice with cold PBS and next resuspended in 100 μL of Annexin V Binding Buffer. Afterwards, the cells were incubated with 5 μL of FITC Annexin V and 5 μL 7-AAD Viability Staining Solution for 15 min at room temperature in the dark. After staining, the events for live, early and late apoptotic cells were counted using a Muse Cell Analyzer (Millipore). The experiments were repeated at least three times.

4.2.6. Immunoblotting

The cells were incubated in solution of the tested compounds (20 μM) for 24 h. After then, the cells were detached by trypsinization, collected in Eppendorf tubes and centrifuged at 2,000 rpm. Next, cell pellets were suspended in 150 μL of complete RIPA Buffer (Thermo Scientific) containing a Halt Protease Inhibitor Cocktail (Thermo Scientific) and Halt Phosphatase Inhibitor Cocktail (Thermo Scientific) along with 0.5 M EDTA and lysed on ice for 20 min on a rocking plate. Subsequently, obtained lysates were sonicated and centrifuged at 10,000 rpm for 10 min at 4° C and the supernatants

were collected for further analysis. The protein concentration was measured using a Micro BCA™ Protein Assay Kit (Thermo Scientific) according to the manufacturer's instruction. Equal amounts of proteins (16 μg) were electrophoresed on SDS-Page gels and transferred onto nitrocellulose membranes. The membranes were blocked in 5% non-fat milk prepared in TPBS (PBS containing 0.1% Tween-20 for 1 h). After blocking, the membranes were incubated with specific primary monoclonal antibodies overnight at 4° C. The next day, membranes were washed in TPBS and incubated with horseradish peroxidase (HRP)-conjugated secondary antibodies for 1 h at room temperature. Finally the membranes were visualized using a ChemiDoc™ XRS+ System (BioRad). The experiments were performed at least three-four times. The densitometric analysis was carried out using ImageJ software (Wayne Rasband, National Institutes of Health, USA).

4.2.7. Time dependent measurement of ROS generation

The cells were incubated with the solutions of the tested compounds for 1, 3, 6, 9, 12 and 24 h. The generation of ROS was assessed immediately according to CellROX® Green Reagent procedure. In addition, the amount of cells in each well was determined using Hoechst 33342 (Molecular Probes™). After time of incubation, the solutions of tested compounds in each well were changed for 100 μL of CellROX Green Reagent (5 μM) and Hoechst 33342 (6 μM) and subsequently cells were incubated for 30 min at 37 ºC. The fluorescence was measured using a multi-plate reader (Synergy 4, Bio Tek) at 485 nm excitation and a 520 nm emission for CellROX Green Reagent and a 345 nm excitation laser and a 485 nm emission filter for Hoechst 33342. The experiments were repeated three to four times. ROS levels were expressed as the percentage of the control cells level.

4.2.8. Statistical analysis

The results are expressed as the mean ± standard deviation (SD) from at least three independent experiments. Statistical analysis was performed using the one-way ANOVA with a Bonferroni post-hoc test (in case of results from progression of cell cycle and Annexin V binding assays) or the two tailed Student's *t*-test (in case of results from ROS level measurement). A p-value of 0.05 or less was considered to be statistically significant. GraphPad Prism 5 software (GraphPad Software, USA) was used for the analysis.

Author contributions

AMW and RM created the research hypothesis; ES carried out the chemical syntheses and designed the experiments, which were supervised by RM; AMW, MK and KM performed the biological tests; AMW, MK, WC and RM wrote and edited the manuscript.

Acknowledgements

This work was supported by the projects of the National Science Centre 2014/13/D/NZ7/00322 (A.M.W.) and 2016/23/N/NZ7/00351 (K.M.). Technical assistance of Klaudia Krzykała is greatly acknowledged.

References

[1] W. Cieslik, R. Musiol, J.E. Nycz, J. Jampilek, M. Vejsova, M. Wolff, et al., Contribution to investigation of antimicrobial activity of styrylquinolines, Bioorg. Med. Chem. 20 (2012) 6960–6968. doi:10.1016/j.bmc.2012.10.027.

[2] A. Kamal, A. Rahim, S. Riyaz, Y. Poornachandra, M. Balakrishna, C.G. Kumar, et al., Regioselective synthesis, antimicrobial evaluation and theoretical studies of 2-styryl quinolines., Org. Biomol. Chem. 13 (2015) 1347–57. doi:10.1039/c4ob02277g.

[3] M. V. Rubtsov, G.N. Pershin, N.A. Yanbuktin, L.A. Pelen-itsina, T.J. Gurevich, N.A. Novitskaya, et al., Derivatives of 2-Styrylquinoline, J. Med. Chem. 2 (1960) 113–131. doi:10.1021/jm50009a001.

[4] J.-F. Mouscadet, D. Desmaële, Chemistry and structure-activity relationship of the styrylquinoline-type HIV integrase inhibitors., Molecules. 15 (2010) 3048–78. doi:10.3390/molecules15053048.

[5] R. Musiol, Quinoline-based HIV integrase inhibitors., Curr. Pharm. Des. 19 (2013) 1835–1849.

[6] R. Musiol, J. Jampilek, V. Buchta, L. Silva, H. Niedbala, B. Podeszwa, et al., Antifungal properties of new series of quinoline derivatives., Bioorg. Med. Chem. 14 (2006) 3592–8. doi:10.1016/j.bmc.2006.01.016.

[7] R. Musiol, J. Jampilek, K. Kralova, D.R. Richardson, D. Kalinowski, B. Podeszwa, et al., Investigating biological activity spectrum for novel quinoline analogues, Bioorg. Med. Chem. 15 (2007) 1280–1288. doi:10.1016/j.bmc.2006.11.020.

[8] R. Musiol, M. Serda, S. Hensel-Bielowka, J. Polanski, Quinoline-based antifungals., Curr. Med. Chem. 17 (2010) 1960–73.

[9] J. Polanski, A. Kurczyk, A. Bak, R. Musiol, Privileged structures - dream or reality: preferential organization of azanaphthalene scaffold., Curr. Med. Chem. 19 (2012) 1921–45.

[10] J. Szczepaniak, W. Cieślik, A. Romanowicz, R. Musioł, A. Krasowska, Blocking and dislocation of Candida albicans Cdr1p transporter by styrylquinolines, Int. J. Antimicrob. Agents. 50 (2017) 171–176. doi:10.1016/j.ijantimicag.2017.01.044.

[11] M. Staderini, S. Aulić, M. Bartolini, H.N.A. Tran, V. González-Ruiz, D.I. Pérez, et al., A Fluorescent Styrylquinoline with Combined Therapeutic and Diagnostic Activities against Alzheimer's and Prion Diseases., ACS Med. Chem. Lett. 4 (2013) 225–9. doi:10.1021/ml3003605.

[12] C.T. Bahner, Effect of compounds related to 4-(p-dimethylaminostyryl) quinoline methiodide on lymphoma 8., Cancer Res. 15 (1955) 588–92.

[13] C.T. Bahner, E.S. Pace, R. Prevost, Quaternary Salts of Styryl Pyridines and Quinolines, J. Am. Chem. Soc. 73 (1951) 3407–3408. doi:10.1021/ja01151a120.

[14] P. Emmelot, C.J. Boss, B.J. Visser, C.T. Bahner, Investigations on growth-inhibitory styrylquinoline compounds and analogues-II, Biochem Pharmacol. 1 (1958) 111–114.

[15] B. Podeszwa, H. Niedbala, J. Polanski, R. Musiol, D. Tabak, J. Finster, et al., Investigating the antiproliferative activity of quinoline-5,8-diones and styrylquinolinecarboxylic acids on tumor cell lines., Bioorg. Med. Chem. Lett. 17 (2007) 6138–41. doi:10.1016/j.bmcl.2007.09.040.

[16] M.A.A. El-Sayed, W.M. El-Husseiny, N.I. Abdel-Aziz, A.S. El-Azab, H.A. Abuelizz, A.A.M. Abdel-Aziz, Synthesis and biological evaluation of 2-styrylquinolines as antitumour agents and EGFR kinase inhibitors: molecular docking study, J. Enzyme Inhib. Med. Chem. 33 (2018) 199–209. doi:10.1080/14756366.2017.1407926.

[17] F.S. Chang, W. Chen, C. Wang, C.C. Tzeng, Y.L. Chen, Synthesis and antiproliferative evaluations of certain 2-phenylvinylquinoline (2-styrylquinoline) and 2-furanylvinylquinoline derivatives, Bioorganic Med. Chem. 18 (2010) 124–133. doi:10.1016/j.bmc.2009.11.012.

[18] C.H. Tseng, C.C. Tzeng, C.C. Chiu, C.Y. Hsu, C.K. Chou, Y.L. Chen, Discovery of 2-[2-(5-nitrofuran-2-yl)vinyl]quinoline derivatives as a novel type of antimetastatic agents, Bioorganic Med. Chem. 23 (2015) 141–148. doi:10.1016/j.bmc.2014.11.015.

[19] A. Mrozek-Wilczkiewicz, E. Spaczynska, K. Malarz, W. Cieslik, M. Rams-Baron, V. Kryštof, et al., Design, Synthesis and In Vitro Activity of Anticancer Styrylquinolines. The p53 Independent Mechanism of Action, PLoS One. 10 (2015) e0142678. doi:10.1371/journal.pone.0142678.

[20] J.N. Fain, Reversal of mitochondrial inhibition of glycolysis by styrylquinolines., Biochem. Pharmacol. 11 (1962) 391–3.

[21] B.A. Foster, H.A. Coffey, M.J. Morin, F. Rastinejad, Pharmacological Rescue of Mutant p53 Conformation and Function, Science (80-.). 286 (1999) 2507–2510. doi:10.1126/science.286.5449.2507.

[22] Y. Luu, J. Bush, K.-J. Cheung, G. Li, The p53 stabilizing compound CP-31398 induces apoptosis by activating the intrinsic Bax/mitochondrial/caspase-9 pathway., Exp. Cell Res. 276 (2002) 214–22. doi:10.1006/excr.2002.5526.

[23] R. Takimoto, W. Wang, D.T. Dicker, F. Rastinejad, J. Lyssikatos, W.S. el-Deiry, The mutant p53-conformation modifying drug, CP-31398, can induce apoptosis of human cancer cells and can stabilize wild-type p53 protein., Cancer Biol. Ther. 1 (2002) 47–55.

[24] J. Mularski, K. Malarz, M. Pacholczyk, R. Musiol, The p53 stabilizing agent CP-31398 and multi-kinase inhibitors. Designing, synthesizing and screening of styrylquinazoline series, Eur. J. Med. Chem. 163 (2019) 610–625. doi:10.1016/j.ejmech.2018.12.012.

[25] A. Mrozek-Wilczkiewicz, D.S. Kalinowski, R. Musiol, J. Finster, A. Szurko, K.

Serafin, et al., Investigating the anti-proliferative activity of styrylazanaphthalenes and azanaphthalenediones., Bioorg. Med. Chem. 18 (2010) 2664–71. doi:10.1016/j.bmc.2010.02.025.

[26] R. Musiol, B. Podeszwa, J. Finster, H. Niedbala, J. Polanski, An Efficient Microwave-Assisted Synthesis of Structurally Diverse Styrylquinolines, Monatshefte Für Chemie - Chem. Mon. 137 (2006) 1211–1217. doi:10.1007/s00706-006-0513-1.

[27] B. Machura, M. Wolff, W. Kowalczyk, R. Musiol, Novel rhenium(V) complexes of 8-hydroxyquinoline derivatives – Synthesis, spectroscopic characterization, X-ray structure and DFT calculations, Polyhedron. 33 (2012) 388–395. doi:10.1016/j.poly.2011.11.051.

[28] B. Machura, M. Wolff, W. Cieślik, R. Musioł, Novel oxorhenium(V) complexes of 8-hydroxyquinoline derivatives – Synthesis, spectroscopic characterization, X-ray crystal structures and DFT calculations, Polyhedron. 51 (2013) 263–274. doi:10.1016/j.poly.2012.12.028.

[29] E.J. Billo, R.P. Graham, P.G. Calway, Hydrolysis of substituted 8-acetoxyquinolines, Talanta. 17 (1970) 180–182. doi:10.1016/0039-9140(70)80123-0.

[30] V. Chobot, S. Drage, F. Hadacek, Redox properties of 8-quinolinol and implications for its mode of action, Nat. Prod. Commun. 6 (2011) 597–602.

[31] E. Spaczyńska, A. Mrozek-Wilczkiewicz, K. Malarz, J. Kos, T. Gonec, E. Al., Design and synthesis of anticancer 1-hydroxynaphthalene-2-carboxanilides with a p53 independent mechanism of action, Sci Rep. in print (2019).

[32] C. Wanka, J.P. Steinbach, J. Rieger, Tp53-induced glycolysis and apoptosis regulator (TIGAR) protects glioma cells from starvation-induced cell death by up-regulating respiration and improving cellular redox homeostasis, J. Biol. Chem. 287 (2012) 33436–33446. doi:10.1074/jbc.M112.384578.

[33] G. Berrozpe, J. Schaeffer, M.A. Peinado, F.X. Real, M. Perucho, Comparative analysis of mutations in the p53 and K-ras genes in pancreatic cancer, Int. J. Cancer. 58 (1994) 185–191. doi:10.1002/ijc.2910580207.

[34] M.S. Redston, C. Caldas, A.B. Seymour, R.H. Hruban, L. da Costa, C.J. Yeo, et al., p53 mutations in pancreatic carcinoma and evidence of common involvement of homocopolymer tracts in DNA microdeletions., Cancer Res. 54 (1994) 3025–33.

[35] B. Ruggeri, S.Y. Zhang, J. Caamano, M. DiRado, S.D. Flynn, A.J. Klein-Szanto, Human pancreatic carcinomas and cell lines reveal frequent and multiple alterations in the p53 and Rb-1 tumor-suppressor genes., Oncogene. 7 (1992) 1503–11.

[36] P.A.J. Muller, K.H. Vousden, P53 Mutations in Cancer, Nat. Cell Biol. 15 (2013) 2–8. doi:10.1038/ncb2641.

[37] W.A. Freed-Pastor, C. Prives, Mutant p53: one name, many proteins., Genes Dev. 26 (2012) 1268–86. doi:10.1101/gad.190678.112.

[38] M. Brázdová, T. Quante, L. Tögel, K. Walter, C. Loscher, V. Tichý, et al., Modulation of gene expression in U251 glioblastoma cells by binding of mutant p53 R273H to intronic and intergenic sequences, Nucleic Acids Res. 37 (2009) 1486–1500.

doi:10.1093/nar/gkn1085.

[39] A. Mrozek-Wilczkiewicz, K. Malarz, M. Rams-Baron, M. Serda, D. Bauer, F.-P. Montforts, et al., Iron Chelators and Exogenic Photosensitizers. Synergy through Oxidative Stress Gene Expression, J. Cancer. 8 (2017) 1979–1987. doi:10.7150/jca.17959.

[40] K. Malarz, A. Mrozek-Wilczkiewicz, M. Serda, M. Rejmund, J. Polanski, R. Musiol, The role of oxidative stress in activity of anticancer thiosemicarbazones, Oncotarget. 9 (2018) 477–486. doi:10.18632/oncotarget.24844.

[41] G. Pastuch-Gawołek, K. Malarz, A. Mrozek-Wilczkiewicz, M. Musioł, M. Serda, B. Czaplinska, et al., Small molecule glycoconjugates with anticancer activity, Eur. J. Med. Chem. 112 (2016) 130–144. doi:10.1016/j.ejmech.2016.01.061.

[42] B. Liu, Y. Chen, D.K. St Clair, ROS and p53: a versatile partnership., Free Radic. Biol. Med. 44 (2008) 1529–35. doi:10.1016/j.freeradbiomed.2008.01.011.

[43] M. Murias, M.W. Luczak, A. Niepsuj, V. Krajka-Kuzniak, M. Zielinska-Przyjemska, P.P. Jagodzinski, et al., Cytotoxic activity of 3,3′,4,4′,5,5′-hexahydroxystilbene against breast cancer cells is mediated by induction of p53 and downregulation of mitochondrial superoxide dismutase, Toxicol. Vitr. 22 (2008) 1361–1370. doi:10.1016/j.tiv.2008.03.002.

[44] G. Pani, B. Bedogni, R. Anzevino, R. Colavitti, B. Palazzotti, S. Borrello, et al., Deregulated manganese superoxide dismutase expression and resistance to oxidative injury in p53-deficient cells., Cancer Res. 60 (2000) 4654–60.

[45] C. Laezza, A. D'Alessandro, L. Di Croce, P. Picardi, E. Ciaglia, S. Pisanti, et al., P53 regulates the mevalonate pathway in human glioblastoma multiforme, Cell Death Dis. 6 (2015) 1–10. doi:10.1038/cddis.2015.279.

[46] H.L. Ko, E.C. Ren, Functional aspects of PARP1 in DNA repair and transcription, Biomolecules. 2 (2012) 524–548. doi:10.3390/biom2040524.

[47] J.M. Rodríguez-Vargas, M.J. Ruiz-Magãa, C. Ruiz-Ruiz, J. Majuelos-Melguizo, A. Peralta-Leal, M.I. Rodríguez, et al., ROS-induced DNA damage and PARP-1 are required for optimal induction of starvation-induced autophagy, Cell Res. 22 (2012) 1181–1198. doi:10.1038/cr.2012.70.

[48] G.V. Chaitanya, A.J. Steven, P.P. Babu, PARP-1 cleavage fragments: signatures of cell-death proteases in neurodegeneration., Cell Commun. Signal. 8 (2010) 31. doi:10.1186/1478-811X-8-31.

[49] C.C. Chang, C.M. Hung, Y.R. Yang, M.J. Lee, Y.C. Hsu, Sulforaphane induced cell cycle arrest in the G2/M phase via the blockade of cyclin B1/CDC2 in human ovarian cancer cells, J. Ovarian Res. 6 (2013) 1–7. doi:10.1186/1757-2215-6-41.

[50] A. Karimian, Y. Ahmadi, B. Yousefi, Multiple functions of p21 in cell cycle, apoptosis and transcriptional regulation after DNA damage, DNA Repair (Amst). 42 (2016) 63–71. doi:10.1016/j.dnarep.2016.04.008.

[51] Y. Gao, The Role of p21 in Apoptosis, Proliferation, Cell Cycle Arrest, and Antioxidant Activity in UVB-Irradiated Human HaCaT Keratinocytes, Med. Sci.

Monit. Basic Res. 21 (2015) 86–95. doi:10.12659/MSMBR.893608.

[52] J.-H. Jeong, S.-S. Kang, K.-K. Park, H.-W. Chang, J. Magae, Y.-C. Chang, p53-Independent Induction of G1 Arrest and p21WAF1/CIP1 Expression by Ascofuranone, an Isoprenoid Antibiotic, through Downregulation of c-Myc, Mol. Cancer Ther. 9 (2010) 2102–2113. doi:10.1158/1535-7163.MCT-09-1159.

[53] M.T. Piccolo, S. Crispi, The Dual Role Played by p21 May Influence the Apoptotic or Anti-Apoptotic Fate in Cancer, J. Can. Res. Updates. 1 (2012) 189–202.

[54] L.Y. Chau, Heme oxygenase-1: Emerging target of cancer therapy, J. Biomed. Sci. 22 (2015) 1–7. doi:10.1186/s12929-015-0128-0.

[55] A. Loboda, M. Damulewicz, E. Pyza, A. Jozkowicz, J. Dulak, Role of Nrf2/HO-1 system in development, oxidative stress response and diseases: an evolutionarily conserved mechanism, Cell. Mol. Life Sci. 73 (2016) 3221–3247. doi:10.1007/s00018-016-2223-0.

[56] S. Bansal, G. Biswas, N.G. Avadhani, Mitochondria-targeted heme oxygenase-1 induces oxidative stress and mitochondrial dysfunction in macrophages, kidney fibroblasts and in chronic alcohol hepatotoxicity, Redox Biol. 2 (2014) 273–283. doi:10.1016/j.redox.2013.07.004.

[57] A.E. Greijer, E. Van Der Wall, The role of hypoxia inducible factor 1 (HIF-1) in hypoxia induced apoptosis, J. Clin. Pathol. 57 (2004) 1009–1014. doi:10.1136/jcp.2003.015032.

[58] G.N. Masoud, W. Li, HIF-1α pathway: Role, regulation and intervention for cancer therapy, Acta Pharm. Sin. B. 5 (2015) 378–389. doi:10.1016/j.apsb.2015.05.007.

[59] D. Liang, M. Yang, B. Guo, L. Yang, J. Cao, X. Zhang, HIF-1α induced by β-elemene protects human osteosarcoma cells from undergoing apoptosis, J. Cancer Res. Clin. Oncol. 138 (2012) 1865–1877. doi:10.1007/s00432-012-1256-5.

[60] T. Schmid, J. Zhou, B. Brüne, HIF-1 and p53: Communication of transcription factors under hypoxia, J. Cell. Mol. Med. 8 (2004) 423–431. doi:10.1111/j.1582-4934.2004.tb00467.x.

[61] A.A. Sablina, A. V Budanov, G. V Ilyinskaya, L.S. Agapova, J.E. Kravchenko, P.M. Chumakov, The antioxidant function of the p53 tumor suppressor., Nat. Med. 11 (2005) 1306–13. doi:10.1038/nm1320.

[62] C.H. Chen, M.L. Lin, P.L. Ong, J.T. Yang, Novel multiple apoptotic mechanism of shikonin in human glioma cells, Ann. Surg. Oncol. 19 (2012) 3097–3106. doi:10.1245/s10434-012-2324-4.

[63] J.T. Yang, Z.L. Li, J.Y. Wu, F.J. Lu, C.H. Chen, An oxidative stress mechanism of shikonin in human glioma cells, PLoS One. 9 (2014). doi:10.1371/journal.pone.0094180.

- Diverse series of styrylquinolines designed and tested for the anticancer activity
- The SAR indicates importance of electron-withdrawing groups and metal chelation site
- The anti-proliferative effect is correlated with the overproduction of intracellular ROS
- The oxidative stress and the ROS-related pathways lead to apoptosis in the p53 independent manner